HHS Public Access

Author manuscript

Am J Surg Pathol. Author manuscript; available in PMC 2020 December 01.

Published in final edited form as:

Am J Surg Pathol. 2019 December ; 43(12): 1682–1692. doi:10.1097/PAS.0000000000001360.

Pericytoma with t(7;12) and *ACTB-GLI1* Fusion: Reevaluation of an Unusual Entity and its Relationship to the Spectrum of *GLI1* Fusion-Related Neoplasms

Darcy A. Kerr, M.D.[1,*], **Andre Pinto, M.D.**[1,*], **Ty K. Subhawong, M.D.**[2], **Breelyn A. Wilky, M.D.**[3], **Matthew P. Schlumbrecht, M.D.**[4], **Cristina R. Antonescu, M.D.**[5], **G. Petur Nielsen, MD**[6], **Andrew E. Rosenberg, M.D.**[1]

[1]Department of Pathology, University of Miami Miller School of Medicine, Miami, FL

[2]Department of Radiology, University of Miami Miller School of Medicine, Miami, FL

[3]Department of Medicine, Division of Hematology-Oncology, University of Miami Miller School of Medicine, Miami, FL

[4]Department of Obstetrics and Gynecology, University of Miami Miller School of Medicine, Miami, FL

[5]Department of Pathology, Memorial Sloan-Kettering Cancer Center, New York, NY

[6]Department of Pathology, Massachusetts General Hospital, Boston, MA

Abstract

The entity “pericytoma with t(7;12)” was described as a rare, distinct perivascular myoid neoplasm provisionally classified within the family of myopericytic tumors that demonstrates t(7;12)(p22;q13) translocation with resultant *ACTB-GLI1* fusion and biologically was felt to behave in an indolent fashion. However, a recent study showed that tumors with this and similar translocations may have variable morphology and immunohistochemical phenotype with inconsistent myopericytic characteristics and a propensity for metastasis, raising questions regarding the most appropriate classification of these neoplasms. Herein, we report 3 additional patients with tumors harboring t(7;12) and *ACTB-GLI1* fusion. The tumors arose in adults and involved the proximal tibia and adjacent soft tissues, scapula and adjacent soft tissues, and ovary. All tumors were composed of round-to-ovoid cells with a richly vascularized stroma with many small, delicate, branching blood vessels, where the neoplastic cells were frequently arranged in a perivascular distribution. Both tumors involving bone showed histologic features of malignancy. By immunohistochemistry, all tested tumors were at least focally positive for SMA (3/3) and CD99 (patchy) (2/2), with variable staining for MSA (2/3), S100 protein (1/3), EMA (2/3), and

Correspondence to: Darcy A. Kerr, MD. Dartmouth-Hitchcock Medical Center, Department of Pathology and Laboratory Medicine, Borwell Level 4, One Medical Center Dr., Lebanon, NH 03756. Phone: 603.650.3808; Fax: 603.650.7214, Darcy.A.Kerr@hitchcock.org.

*These authors contributed equally to the work

Current affiliations:

Darcy A. Kerr, M.D.: Department of Pathology, Dartmouth-Hitchcock Medical Center and Geisel School of Medicine at Dartmouth, Lebanon, NH

Breelyn A. Wilky, M.D.: Department of Medicine, University of Colorado School of Medicine, Aurora, CO.

Disclosures: The authors have no relevant conflicts of interest to disclose.

pan-keratin (1/3); all were negative for desmin and WT1 (0/3). The two patients with bone tumors developed metastases (27 and 84 months after diagnosis). Whether these tumors are best classified as malignant myopericytoma variants or an emerging translocation-associated sarcoma of uncertain differentiation remains to be fully clarified; however, our study further documents the potential for these tumors to behave in an aggressive fashion, sometimes over a prolonged clinical course.

Keywords

Pericytoma; Myopericytoma; Sarcoma; GLI1; ACTB

INTRODUCTION

The entity “pericytoma with t(7;12)” was described as a rare perivascular myoid neoplasm provisionally classified as a discrete subgroup within the family of myopericytic tumors. Initially described by Dahlén et al. in 2004 as a group of soft tissue neoplasms with distinctive pericytic features that shared the t(7;12)(p22;q13) translocation by cytogenetic analysis, the resultant unique *ACTB-GLI1* fusion was considered the driving genetic abnormality. Based on the first 7 cases reported in the literature, the histological features were interpreted as benign and no aggressive biologic behavior was documented clinically with a mean follow up of 60 months (range 6–168).[1–3] However, recently, 6 tumors with a round to epithelioid, nested morphology harboring *GLI1* gene fusions, including 4 fused to *ACTB*, 1 to *MALAT1* and 1 to *PTCH1* gene have been reported.[4] In this series, the morphologic and immunophenotypic evidence of myopericytic lineage of the tumors was not convincing, and the tumors demonstrated significant metastatic potential.[4] The constellation of reported findings raises questions about how to best classify these neoplasms and whether tumors with *ACTB-GLI1* fusion represent multiple distinct entities or different manifestations of a spectrum of tumors with variable pericytic nature and biologic potential. Herein, we describe 3 additional cases of neoplasms with *ACTB-GLI1* fusion and expand upon the morphologic, immunophenotypic, and clinical behavior of this evolving entity.

MATERIALS AND METHODS

The study was approved by the Institutional Review Board (IRB). Cases with *ACTB-GLI1* gene fusion were identified both prospectively (cases #1 and 3) and retrospectively by searching the files of the senior author (A.E.R., case #2). All tumors were routinely processed and embedded in paraffin. Immunohistochemistry was performed on 4-μm-thick formalin-fixed, paraffin-embedded (FFPE) tissue according to standard techniques. Hematoxylin and eosin-stained slides and available immunohistochemical stains were reviewed. Clinical information was obtained by review of the electronic medical records and contacting the treating physicians.

Molecular Studies

Nucleic acids were extracted and libraries were prepared from unstained FFPE slides of non-decalcified, tumor-bearing tissue. Two cases (cases #1 and 3) underwent analysis by a next-generation sequencing (NGS)-based assay that interrogates 406 genes by DNA sequencing, select introns of 31 genes involved in rearrangements, and 265 genes by RNA sequencing (FoundationOne®, Cambridge, MA). In one case (case #2), a clinically-validated, laboratory-developed Anchored Multiplex PCR (AMP)-based assay was utilized to interrogate for targeted fusion transcripts involving 51 genes by NGS.[5] ArcherDx FusionPlex® Solid Tumor and Sarcoma kits (ArcherDx, Boulder, CO) were utilized to prepare a custom library which was sequenced on an Illumina NextSeq instrument (Illumina®, San Diego, CA) and analyzed by a laboratory-developed algorithm. Interphase fluorescence in situ hybridization (FISH) was performed on 4-μm-thick FFPE tissue sections. *EWSR1* FISH was conducted in two cases (cases #1 and 2, Vysis LSI EWSR1 Dual Color, Break Apart Probe, Abbott Laboratories, Abbott Park, IL). In one case (case #1), confirmatory FISH was performed with custom bacterial artificial chromosome (BAC) probes for *GLI1* and *ACTB* as per a previously described protocol.[4] For the ovarian case (case #3), FISH was performed with a break-apart probe for *JAZF1* by a laboratory-developed test at a reference center (Mayo Medical Laboratories, Rochester, MN).

RESULTS

Patient 1

A 57-year-old woman presented with a 3-month history of a mass in her right leg. The mass was not painful and physical exam revealed fullness to the right proximal tibia region and a few prominent, dilated veins in the overlying soft tissues.

Magnetic resonance imaging (MRI) revealed a 1.9 × 1.8 × 2.3 cm intraosseous tumor of the medial proximal tibia associated with a 9.8 × 3.8 × 4.5 cm posterior soft tissue mass involving the flexor compartment (Figure 1A). Positron emission tomography-computed tomography (PET-CT) scan showed avid FDG uptake in both components. An incisional biopsy was performed and was interpreted as an undifferentiated small round cell sarcoma, Ewing sarcoma-like in nature, with an unknown, non-*EWSR1* translocation.

Staging studies revealed no evidence of metastatic disease. Chemotherapy was performed and consisted of 4 cycles of vincristine, actinomycin, and ifosfamide (VAI). After neoadjuvant therapy, a radiograph of the tibia showed a lytic lesion with non-sclerotic margin and focal high-grade endosteal scalloping (Figure 1B). While the overall tumor size was slightly increased on MRI, the intra-osseous component showed non-enhancing, hemorrhagic, cystic components indicative of treatment effect.

The patient underwent wide excision of the right proximal tibia and soft tissue mass with total knee reconstruction. Gross examination revealed a 5.5 × 4.0 × 3.0 cm soft, red-white, hemorrhagic, predominantly cystic intraosseous tumor with white fibrous septae centered within the tibial epiphysis and metaphysis. The tumor destroyed the posterior cortex and formed a 10.0 × 4.0 × 3.5 cm soft pink-tan fleshy soft tissue component (Figure 2A). It involved the medullary cavity, permeated the trabecular bone, transgressed the cortex

eliciting subperiosteal reactive woven bone formation, and infiltrated the neighboring soft tissue (Figure 2B). The tumor demonstrated multinodular and focally perivascular growth with a conspicuous “hemangiopericytoma”-like vasculature. The neoplastic cells were small and round to ovoid with oval to irregular nuclei, vesicular chromatin with small nucleoli, and scant clear to pale eosinophilic cytoplasm (Figure 2C). Vascular invasion was present with prominent subendothelial tumor proliferation. Mitoses numbered 5/10 high power fields (HPF). Approximately 40% of the tumor was necrotic and 60% was viable. Most of the necrotic area was represented by cystic change within the intra-osseous component, while the soft tissue component was predominantly viable. The surgical resection margins were negative for tumor.

Immunohistochemical stains showed that the tumor cells were positive for FLI-1 (strong, diffuse), SMA (focal; Figure 2D), MSA (rare cells), h-caldesmon (rare cells), synaptophysin (rare cells), EMA (weak, focal), and CD99 (weak, focal, cytoplasmic). Stains for CD31 and CD34 highlighted the prominent thin-walled vasculature within the tumor, and the neoplastic cells were negative. The tumor cells were additionally negative for S100 protein, pan-keratin, desmin, collagen type IV, WT1 (c-terminus and n-terminus), TdT, HMB45, and CD10. The proliferative index as estimated by a Ki67 nuclear labeling index was approximately 35%.

Conventional cytogenetics failed to grow metaphase cells suitable for chromosomal analysis. FISH was negative for rearrangement of *EWSR1*. An NGS-based assay (FoundationOne®, Cambridge, MA) revealed 3 genetic abnormalities: *ACTB-GLI1* rearrangement, *JAK2* G571S mutation, and *NOTCH2* P6fs*27. Tumor mutational burden was low (5 mutations/Mb). FISH studies confirmed gene rearrangements in both *ACTB* and *GLI1* genes (Figure 2E–F).

After surgery, Ewing-family salvage chemotherapy was discontinued. Subsequently, 27 months after diagnosis the patient developed chest wall pain and radiographs revealed a destructive lesion of the 8th rib. Needle biopsy and wide resection of the rib confirmed metastatic sarcoma with features similar to those seen in the tibial tumor.

Patient 2

A 62-year-old man presented with a palpable mass of his right shoulder. MRI demonstrated a 6 × 8 × 10 cm solid mass arising from the body of the right scapula with associated bony destruction. A core needle biopsy of the mass was performed and was interpreted as representing an atypical small round cell neoplasm, favored to be malignant, and possibly representing Ewing sarcoma. Staging CT scans of the chest, abdomen, and pelvis revealed no evidence of metastatic disease.

Resection of the scapula mass revealed a 7.5 cm tumor that diffusely infiltrated the bone; there was prominent vascular invasion and multiple satellite nodules separate from the main mass. The tumor was composed of small round cells with round to oval nuclei, fine chromatin, and clear to eosinophilic cytoplasm. In areas the neoplastic cells had distinct cytoplasmic borders and formed gland-like structures. The stroma showed focal myxoid change and prominent, delicate vasculature. Mitoses were rare (1/50 HPF) and no necrosis

was identified. Tumor was present at the lateral bone margin. Immunohistochemical studies showed that the tumor cells were positive for SMA, MSA, vimentin, and BCOR (weak). They showed only cytoplasmic staining for CD99 and were negative for FLI-1, desmin, calponin, myogenin, MyoD1, ETV4, WT1, CD45, pan-keratin, MNF116, EMA, S100 protein, synaptophysin, and chromogranin. FISH was negative for rearrangement of *EWSR1*. Despite relatively bland cytologic features and low mitotic activity, the tumor was classified as a low to intermediate grade sarcoma due to the prominent vascular invasion and bony infiltration.

The patient received postoperative radiation therapy and was free of disease until 7 years after initial presentation when a left lung metastasis was detected on surveillance imaging. The sub-centimeter metastasis was resected and histologically showed morphologic features identical to those seen in the primary scapula tumor. Two years later (9 years after initial diagnosis), he developed a right-sided lung metastasis and had this surgically resected along with the right clavicle. Fifteen years after initial diagnosis, the patient developed a mass in the right thigh, and core biopsy demonstrated a histologically identical metastatic small round cell sarcoma. Upon resection, the tumor predominantly involved skeletal muscle of the thigh but focally involved the cortex of the femur (Figure 3A). As with prior specimens, the sarcoma maintained the same histologic features (Figure 3B–C) and overall immunophenotype, with diminution of the degree of SMA positivity (focal as compared to the more extensive staining seen previously). The clinically-validated, laboratory-developed AMP-based assay revealed an *ACTB-GLI1* fusion.

Patient 3

A 41-year-old pre-menopausal woman was referred because of an incidentally discovered left ovarian cyst. She denied abnormal vaginal bleeding or discharge, pelvic or abdominal pain, bloating, change in urinary or bowel habits, and change in appetite or energy.

Initially the cyst measured 6.0 cm by imaging, and surveillance was recommended with yearly ultrasound. Subsequent imaging studies revealed a slight increase in size (6.5 cm and 7.4 cm in 2 consecutive years). The last MRI scan showed a solid and cystic enhancing heterogeneous mass within the left adnexa with some internal restricted diffusion, measuring 5.5 × 7.4 × 5.5 cm. At that time, the concern for malignancy prompted exploratory laparotomy with left salpingo-oophorectomy. Intraoperative frozen section reported granulosa cell tumor, so a completion total abdominal hysterectomy, right salpingo-oophorectomy, and infracolic omentectomy were performed. Operative findings were notable for a small uterus with a relatively immobile pelvic mass posteriorly, without evidence of disease elsewhere. Extensive adhesions in the pelvis between the uterus, left pelvic mass, rectum, and left pelvic sidewall were present. There was partial rupture of the tumor intraoperatively.

Gross examination showed a partially disrupted 7.0 × 4.5 × 3.0 cm left ovarian mass with an uninvolved, smooth surface. On sectioning the mass was solid and cystic, white-brown with few areas of necrosis. No residual normal ovarian stroma could be identified. Histologic examination showed that the tumor was composed of uniform, ovoid cells with alternating areas of hypercellularity and edema (Figure 4A–B). The stroma was remarkable for a

prominent vascular tree consisting of small-diameter, interconnecting, and delicate blood vessels. Regional necrosis was present, but mitotic activity was low (1 mitosis per 50 HPF).

By immunohistochemistry, the lesional cells expressed pan-keratin, EMA, SMA (focal, Figure 4C), S100 protein (focal, Figure 4D) and CD10 but were negative for pan-cytokeratin, WT1, PAX8, SF-1, inhibin, synaptophysin, SALL4, CD31, nuclear beta-catenin, ALK, desmin, HMB45 and Melan A. The Ki67 labeling index was approximately 1%.

Given the failure to establish a definitive line of differentiation immunohistochemically, molecular studies were pursued with NGS-based sequencing (FoundationOne®, Cambridge, MA). The tumor showed a low mutation burden (2 mutations/Mb), and the only definitive genomic alteration identified was t(7; 12) with *GLI1-ACTB* rearrangement.

The clinical team opted for surveillance without further therapeutic intervention. The patient is being followed and is currently free of disease 14 months after surgery.

DISCUSSION

We have presented 3 tumors composed of round-to-ovoid cells associated with a delicate vasculature that immunophenotypically show at least focal myogenic differentiation (SMA positivity seen in all cases, being focal in 2) and genetically harbor *ACTB-GLI1* fusion (demographic, histologic, and immunophenotypic findings are summarized in Tables 1–2). Whether these tumors are best classified of variants of “pericytoma with t(7;12)” or a novel soft tissue neoplasm with metastatic potential is open to debate.

Myopericytomas are benign perivascular myoid tumors of a family that includes myofibroma, infantile myofibroma or myofibromatosis, angioleiomyoma, and glomangiopericytoma/glomus tumor. The line of differentiation is the myopericyte, a cell with combined features of pericytes and smooth muscle cells thought to represent a transitional form between the two cell lineages.[6] In addition to participating in angiogenesis and blood pressure control, pericytes are thought to play important roles in tumor formation, growth, angioinvasion, and metastasis. Additionally, pericytes are hypothesized to be a type of perivascular stem cell that can differentiate along numerous mesenchymal lineages.[7] Immunophenotypically, myopericytomas are generally characterized by positivity for SMA, h-caldesmon, MSA, and collagen type IV and no staining for desmin or S100 protein. Proliferative activity in myopericytoma is usually low (<2/10 HPF).[6,8]

Postulated to be a distinct subset of myopericytoma is the entity provisionally named “pericytoma with t(7;12)” which harbors a translocation involving *ACTB* and *GLI*. In the initial series of 5 cases, the tumor was described as exhibiting distinctive histology, composed of multiple lobules of small ovoid and spindle cells often having a perivascular pattern with groups of tumor cells surrounded by thin-walled vessels and demonstrating an infiltrative growth pattern.[1] The spindle cells had scant eosinophilic cytoplasm, ovoid-to-tapered nuclei, vesicular chromatin, and small nucleoli with no significant cytologic atypia, necrosis, or mitotic activity. Immunohistochemically, they were positive for SMA and negative for S100 protein[1] Subsequently, 3 additional cases[2,3,9] were described with similar

morphologic and immunophenotypic features, although 1 case was reported to be negative for SMA.[3] The cumulative limited published clinical follow-up did not indicate aggressive behavior, with a mean follow up of 60 months (range 6–168).[1–3,9] Gathering additional clinical follow up by contacting the prior authors for our study did not change this number significantly (mean follow up of 65 months (range 6–204)), because while 2 historical case had 4 additional cumulative years of disease-free follow-up, another case previously too recent to include in follow-up now has limited disease-free follow-up of 2 years (see Table 3: patients 1, 5, and 12, respectively).

In contrast, Antonescu et al. recently described 6 tumors with round to epithelioid phenotype showing *GLI1* fusions (4 with *ACTB-GLI1*, 1 with *GLI1-MALAT1*, and 1 with *GLI1-PTCH1*) that exhibited significant metastatic potential.[4] Immunophenotypically, most of the tumors were strongly positive for S100 protein (4/6) and all were negative for SMA and EMA. Given an immunophenotype not typical for pericytic lineage, the authors hypothesized that the tumors potentially either represent a novel soft tissue sarcoma or an unusual manifestation of the previously described *GLI1* fusion-related neoplasms, and they proposed the provisional terminology: “malignant epithelioid neoplasm with *GLI1* fusions.” The 3 patients for whom clinical follow up was available (mean of 50 months) all demonstrated metastatic disease within lymph nodes with one patient additionally developing lung metastasis.[4]

Our findings help to partially bridge information between these prior studies. All tumors in our cohort were at least focally positive for SMA and demonstrated perivascular growth that may indicate morphologic evidence of myopericytic differentiation. However, 2 of our tumors (both arising in bone) were classified as malignant based on local infiltration and vascular invasion and subsequently metastasized (patient #1 to bone at 27 months, patient #2 to lung at 7 years and soft tissue/bone at 15 years), similar to the biologic potential demonstrated in the *GLI1*-rearranged cohort reported by Antonescu et al. Additionally, 1 of our cases (patient #3, with tumor involving the ovary) showed S100 protein reactivity, a finding that characterized the latter *GLI1*-rearranged tumors, and it is the only tumor in our cohort that so far has not metastasized; however, clinical follow-up is short. Although the earlier series of *GLI1-ACTB* tumors reported as pericytoma with t(7;12) were described as tumors composed of spindle-to-ovoid cells, the illustrations show that they are predominantly ovoid and are morphologically similar to the tumors in the series by Antonescu and our cases. Based on review of the available literature, histologic classification of these tumors as benign or malignant has been inferred from available clinical follow-up. Taking together all previously and currently reported tumors with *GLI1-ACTB* translocation, all have lacked significant nuclear atypia or pleomorphism and mitotic activity has been relatively low (1–5 mitoses/10 HPF). Most tumors have displayed infiltrative growth, and approximately half demonstrate focal myxoid stroma. Focal necrosis has occasionally been noted in primary tumors (20%, n=3/15). Tumors have shown a 2:1 female predominance and have affected patients across a large age range (9–79 years, mean 39) with an average size of 5.5 cm (range 0.8–15.0). The tumors have arisen more frequently in soft tissue than bone (4:1) and most commonly have involved the somatic soft tissue (n=4; specific sites: calf, thigh, foot, chest wall), tongue (n=3), and bone (n=3) with occasional

cases reported in the stomach (n=2), ovary (n=2), and retroperitoneum (n=1). Features of previously and currently reported cases are summarized in Table 3.

While the relatively small number of reported cases precludes definitively answering the question of whether *GLI1-ACTB* fusion in these round and ovoid cell tumors defines a specific entity or whether it is an alteration seen in several different types of neoplasms, it may be informative to attempt to understand how these cases were classified before the molecular information was known. In the initial series, it is largely unclear as the cases were selected based on cytogenetic findings.[1] However, interestingly, 1 of these 5 initial cases had previously been reported as an "infantile hemangiopericytoma," characterized as SMA negative with mitoses up to 9/10 HPF in the original case report.[10] The subsequently reported case, by Bridge et al, was considered a low-grade malignant neoplasm of uncertain histogenesis by core biopsy, but later reclassified on resection, noting, "cytogenetic and molecular analyses were useful, if not essential, in classifying this rare diagnostic entity."[2] Next, Castro and colleagues considered angiomatoid fibrous histiocytoma for the pediatric gastric tumor they reported, but *EWSR1* FISH was negative, and the authors remarked, "the unusual location and nonspecific morphology made the differential diagnosis quite difficult, making genetic and molecular analyses imperative for the correct diagnosis."[3] Within the cohort of 6 *GLI1* fusion related neoplasms reported by Antonescu et al, the most common initial diagnosis was myoepithelial carcinoma (n=3), with 1 case initially diagnosed as an epithelioid schwannoma until it metastasized. One case was considered an unusual pericytic tumor despite positivity for S100 protein and negativity for SMA because of its morphologic resemblance to cellular glomus tumor and the presence of *ACTB-GLI1*, so it is difficult to be sure how this case would have been characterized without the genetic information.[4] Koh and colleagues considered a range of primary ovarian neoplasms for their case and also noted the importance of molecular findings for its classification, given the rarity of tumors with *ACTB-GLI1* compared to others in the differential diagnosis as well as the morphologic, immunophenotypic, and clinical variability in the previously reported cases.[9] For our cases, both tumors involving bone were considered to be Ewing-like sarcomas; however the case with more prominent myogenic differentiation (case #2) was interpreted as a malignant glomus tumor prior to NGS. Given the above findings, a pattern seems to emerge: many - if not most - of these tumors do not seem diagnosable as (myo)pericytic based on morphology and immunohistochemistry alone, lending uncertainty to their histogenesis.

While the *ACTB-GLI1* fusion has not yet been reported outside of the above context (pericytoma with t(7;12) and malignant epithelioid neoplasm with *GLI1* fusions), the other 2 fusions reported by Antonsecu have been identified in other neoplasms: *GLI1-MALAT1* in gastroblastoma,[11] a tumor with some morphologic and immunophenotypic overlap with current tumors, and plexiform fibromyxoma,[12] a seemingly entirely distinct tumor. Based on all of the reported cases, *ACTB-GLI1* fusions may be characteristic of one entity, but *GLI1*-rearranged tumors with different fusion partners may represent related but distinct neoplasms.

The differential diagnosis for mesenchymal neoplasms with *ACTB-GLI1* and related gene fusions differs based upon a variety of factors, including their morphologic,

immunohistochemical, and clinical manifestations. Our first two tumors were malignant small round cell tumors involving bone, with an associated differential diagnosis broadly including small round cell sarcomas, melanoma, small cell carcinoma, and rhabdomyosarcoma. The latter 3 possibilities were excluded by immunohistochemistry. Among small round cell sarcomas, Ewing sarcoma was a principal diagnostic consideration in each instance. Morphologically, however, both tumors possessed a perivascular growth pattern and lacked a “two-cell” population that is common in Ewing sarcoma (comprised of cells that are viable and others that are necrotic or apoptotic). Immunohistochemically, while both tumors were strongly positive for FLI-1 on initial biopsy, they showed variable reactivity for CD99 (predominantly cytoplasmic) and, importantly, both were negative for *EWSR1* rearrangement by FISH. An increasing number of Ewing-like round cell sarcomas or undifferentiated sarcomas with round cell phenotype have been recognized, including sarcomas associated with translocations of *BCOR-CCNB3* and *CIC-DUX4* or *CIC-FOXO4*.[13,14] The morphology of these sarcomas varies, and may include a spindle cell component, epithelioid or rhabdoid cells, myxoid stroma, and a staghorn-like vascular tree. Immunohistochemically, these sarcomas may demonstrate variable patterns of CD99 positivity, unlike the diffuse, strong, membranous pattern characteristic of Ewing sarcoma. However, many are positive for WT1, while both of our cases were negative for WT1, and the case that was tested for BCOR immunohistochemistry (case #2) was only weakly reactive. Additional clues to the diagnosis in our cases include the delicate branching vasculature with perivascular arrangement of tumor cells and the variable positivity for myogenic markers (SMA, MSA, and h-caldesmon); however, genetic analysis has proven to be a critical tool in the classification of these malignant small round cell neoplasms.

For our third tumor involving the ovary, the differential diagnosis included tumors that more frequently involve the adnexa, such as sex-cord stromal tumors, low-grade endometrioid stromal sarcoma, and less likely, other tumors of mesenchymal origin (such as epithelioid smooth muscle neoplasms). A single prior case of pericytoma with t(7;12) arising in the ovary has been recently described.[9] This index case consisted of an 11-year old child presenting with a 16.5 cm adnexal mass. Similar to our two tumors arising in bone, the lack of pertinent immunohistochemical staining that would support any definitive line of differentiation argued against most of these diagnoses for the ovarian tumor. Interestingly, the tumor was diffusely positive for CD10, which raised the possibility of a low-grade endometrioid stromal tumor, however FISH studies for translocation involving the *JAZF1* gene (which is seen in such neoplasms), were negative.

Molecularly, the t(7;12)(p22;q13) translocation leads to fusion of the *GLI1* oncogene and *ACTB*, whereby the universally expressed *ACTB* gene promoter drives increased *GLI1* expression; this leads to transcriptional activation and reregulation of downstream target genes thereby affecting cell-cycle regulation, cell adhesion, apoptosis, signal transduction, and cell proliferation.[1,2,15] Activation of *GLI1* oncogene is important in the *sonic hedgehog* (SHH) signaling pathway, and *GLI1* is amplified in many human malignancies, including glioblastoma and rhabdomyosarcoma.[1,15,16] Targeting the SHH-GLI pathway is considered a desirable and potentially feasible therapeutic approach for a variety of different malignancies.[16]

While in two of our tumors *GLI1-ACTB* rearrangement was the only abnormal genetic abnormality detected by NGS, the tibial tumor (patient #1) also demonstrated mutations in *Notch2* and *JAK2*. Notch2 is a member of the Notch family of receptors that play a role in developmental processes, homeostasis, and cell-fate determination, and it can act as either an oncogene or, less commonly, a tumor suppressor gene.[17–20] The *NOTCH2* p6fs*27 deletion is a frameshift mutation that alters or disrupts the ankyrin repeat region (amino acids 1876–2041), predicted to be an inactivating mutation.[21–23] Notch2 protein inactivating mutations are seen in squamous cell carcinomas of various anatomical sites and bladder carcinomas.[18,20,24] Lack of Notch signaling has been implicated in epithelial-to-mesenchymal transition,[17,18] and thus this *NOTCH2* mutation may have contributed to the malignant phenotype in this myopericytoma. *JAK2* encodes Janus kinase 2, a tyrosine kinase that regulates signaling initiated by cytokines and growth factors and is often mutated in hematopoietic and lymphoid malignancies.[25] Most mutations occur at V617, but G571S has been observed in patients with myeloproliferative neoplasms[26] and erythrocytosis.[27] However, available evidence suggests that the G571S mutation is not a JAK2-activating mutation,[26] and thus this finding may not be a significant contributor to the malignant phenotype of this case.

In summary, we describe 3 new cases of mesenchymal neoplasms with translocations involving *ACTB* and *GLI1* genes, and results support emerging evidence that tumors with this genetic abnormality have the potential to behave in a biologically aggressive fashion. Whether these tumors are most appropriately classified as (malignant) pericytoma variants or novel sarcomas of uncertain histogenesis still remains unclear. However, it is our opinion that it is feasible that all of these tumors represent a morphologic spectrum with variable degrees of pericytic differentiation, immunohistochemical findings, and metastatic potential. Interestingly, the clinical course of patients with metastatic disease is prolonged with metastases not developing for many years in some patients. This study expands the clinicopathologic and molecular data for this exceedingly rare group of tumors and will contribute to further understanding of tumors harboring *ACTB-GLI* translocations.

Acknowledgements

The authors would like to thank Drs. Derrick Lian, Julia Bridge, and Fredrik Mertens for providing additional clinical follow-up on their previously published cases.

REFERENCES

1. Dahlen A, Fletcher CD, Mertens F, et al. Activation of the GLI oncogene through fusion with the beta-actin gene (ACTB) in a group of distinctive pericytic neoplasms: pericytoma with t(7;12). Am J Pathol. 2004;164(5):1645–1653. [PubMed: 15111311]
2. Bridge JA, Sanders K, Huang D, et al. Pericytoma with t(7;12) and ACTB-GLI1 fusion arising in bone. Hum Pathol. 2012;43(9):1524–1529. [PubMed: 22575261]
3. Castro E, Cortes-Santiago N, Ferguson LM, Rao PH, Venkatramani R, Lopez-Terrada D. Translocation t(7;12) as the sole chromosomal abnormality resulting in ACTB-GLI1 fusion in pediatric gastric pericytoma. Hum Pathol. 2016;53:137–141. [PubMed: 26980027]
4. Antonescu CR, Agaram NP, Sung Y-S, Zhang L, Swanson D, Dickson BC. A Distinct Malignant Epithelioid Neoplasm With GLI1 Gene Rearrangements, Frequent S100 Protein Expression, and Metastatic Potential: Expanding the Spectrum of Pathologic Entities With ACTB/MALAT1/PTCH1-GLI1 Fusions. Am J Surg Pathol. 2018;42(4):553–560. [PubMed: 29309307]

5. Zheng Z, Liebers M, Zhelyazkova B, et al. Anchored multiplex PCR for targeted next-generation sequencing. Nat Med. 2014;20(12):1479–1484. [PubMed: 25384085]
6. Mentzel T, Dei Tos AP, Sapi Z, Kutzner H. Myopericytoma of skin and soft tissues: clinicopathologic and immunohistochemical study of 54 cases. Am J Surg Pathol. 2006;30(1):104–113. [PubMed: 16330949]
7. Mravic M, Asatrian G, Soo C, et al. From pericytes to perivascular tumours: correlation between pathology, stem cell biology, and tissue engineering. Int Orthop. 2014;38(9):1819–1824. [PubMed: 24566993]
8. Mentzel T, Bridge JA. Myopericytoma, including myofibroma In: Fletcher CD, Bridge JA, Hogendoorn PCW, Mertens F, eds. WHO Classification of Tumors of Soft Tissue and Bone. Vol 4th 4th ed. Lyon: International Agency for Research on Cancer; 2013:118–120.
9. Koh NWC, Seow WY, Lee YT, Lam JCM, Lian DWQ. Pericytoma With t(7;12): The First Ovarian Case Reported and a Review of the Literature. Int J Gynecol Pathol. 8 2018. doi:10.1097/PGP.0000000000000542
10. Perez-Atayde AR, Kozakewich HW, McGill T, Fletcher JA. Hemangiopericytoma of the tongue in a 12-year-old child: ultrastructural and cytogenetic observations. Hum Pathol. 1994;25(4):425–429. [PubMed: 8163277]
11. Graham RP, Nair AA, Davila JI, et al. Gastroblastoma harbors a recurrent somatic MALAT1-GLI1 fusion gene. Mod Pathol. 2017;30(10):1443–1452. [PubMed: 28731043]
12. Spans L, Fletcher CD, Antonescu CR, et al. Recurrent MALAT1-GLI1 oncogenic fusion and GLI1 up-regulation define a subset of plexiform fibromyxoma. J Pathol. 2016;239(3):335–343. [PubMed: 27101025]
13. Antonescu CR, Owosho AA, Zhang L, et al. Sarcomas With CIC-rearrangements Are a Distinct Pathologic Entity With Aggressive Outcome: A Clinicopathologic and Molecular Study of 115 Cases. Am J Surg Pathol. 2017;41(7):941–949. [PubMed: 28346326]
14. Matsuyama A, Shiba E, Umekita Y, et al. Clinicopathologic Diversity of Undifferentiated Sarcoma With BCOR-CCNB3 Fusion: Analysis of 11 Cases With a Reappraisal of the Utility of Immunohistochemistry for BCOR and CCNB3. Am J Surg Pathol. 2017;41(12):1713–1721. [PubMed: 28877060]
15. Dahlen A, Mertens F, Mandahl N, Panagopoulos I. Molecular genetic characterization of the genomic ACTB-GLI fusion in pericytoma with t(7;12). Biochem Biophys Res Commun. 2004;325(4):1318–1323. [PubMed: 15555571]
16. Rimkus TK, Carpenter RL, Qasem S, Chan M, Lo HW. Targeting the Sonic Hedgehog Signaling Pathway: Review of Smoothened and GLI Inhibitors. Cancers. 2016;8(2). doi:10.3390/cancers8020022
17. Andersson ER, Lendahl U. Therapeutic modulation of Notch signalling--are we there yet? Nat Rev Drug Discov. 2014;13(5):357–378. [PubMed: 24781550]
18. Maraver A, Fernandez-Marcos PJ, Cash TP, et al. NOTCH pathway inactivation promotes bladder cancer progression. J Clin Invest. 2015;125(2):824–830. [PubMed: 25574842]
19. Wu WR, Zhang R, Shi XD, Yi C, Xu LB, Liu C. Notch2 is a crucial regulator of self-renewal and tumorigenicity in human hepatocellular carcinoma cells. Oncol Rep. 2016;36(1):181–188. [PubMed: 27221981]
20. Zou Y, Fang F, Ding YJ, et al. Notch 2 signaling contributes to cell growth, anti-apoptosis and metastasis in laryngeal squamous cell carcinoma. Mol Med Rep. 2016;14(4):3517–3524. [PubMed: 27572051]
21. Bea S, Valdes-Mas R, Navarro A, et al. Landscape of somatic mutations and clonal evolution in mantle cell lymphoma. Proc Natl Acad Sci U S A. 2013;110(45):18250–18255. [PubMed: 24145436]
22. McDaniell R, Warthen DM, Sanchez-Lara PA, et al. NOTCH2 mutations cause Alagille syndrome, a heterogeneous disorder of the notch signaling pathway. Am J Hum Genet. 2006;79(1):169–173. [PubMed: 16773578]
23. Cosmic. COSMIC - Catalogue of Somatic Mutations in Cancer. http://cancer.sanger.ac.uk/cosmic. Published May 15, 2019 Accessed May 21, 2019.

24. Wang NJ, Sanborn Z, Arnett KL, et al. Loss-of-function mutations in Notch receptors in cutaneous and lung squamous cell carcinoma. Proc Natl Acad Sci U S A. 2011;108(43):17761–17766. [PubMed: 22006338]

25. Jatiani SS, Baker SJ, Silverman LR, Reddy EP. Jak/STAT pathways in cytokine signaling and myeloproliferative disorders: approaches for targeted therapies. Genes Cancer. 2010;1(10):979–993. [PubMed: 21442038]

26. Milosevic Feenstra JD, Nivarthi H, Gisslinger H, et al. Whole-exome sequencing identifies novel MPL and JAK2 mutations in triple-negative myeloproliferative neoplasms. Blood. 2016;127(3):325–332. [PubMed: 26423830]

27. Bahar B, Barton K, Kini AR. The role of the Exon 13 G571S JAK2 mutation in myeloproliferative neoplasms. Leuk Res Rep. 2016;6:27–28. [PubMed: 27924280]

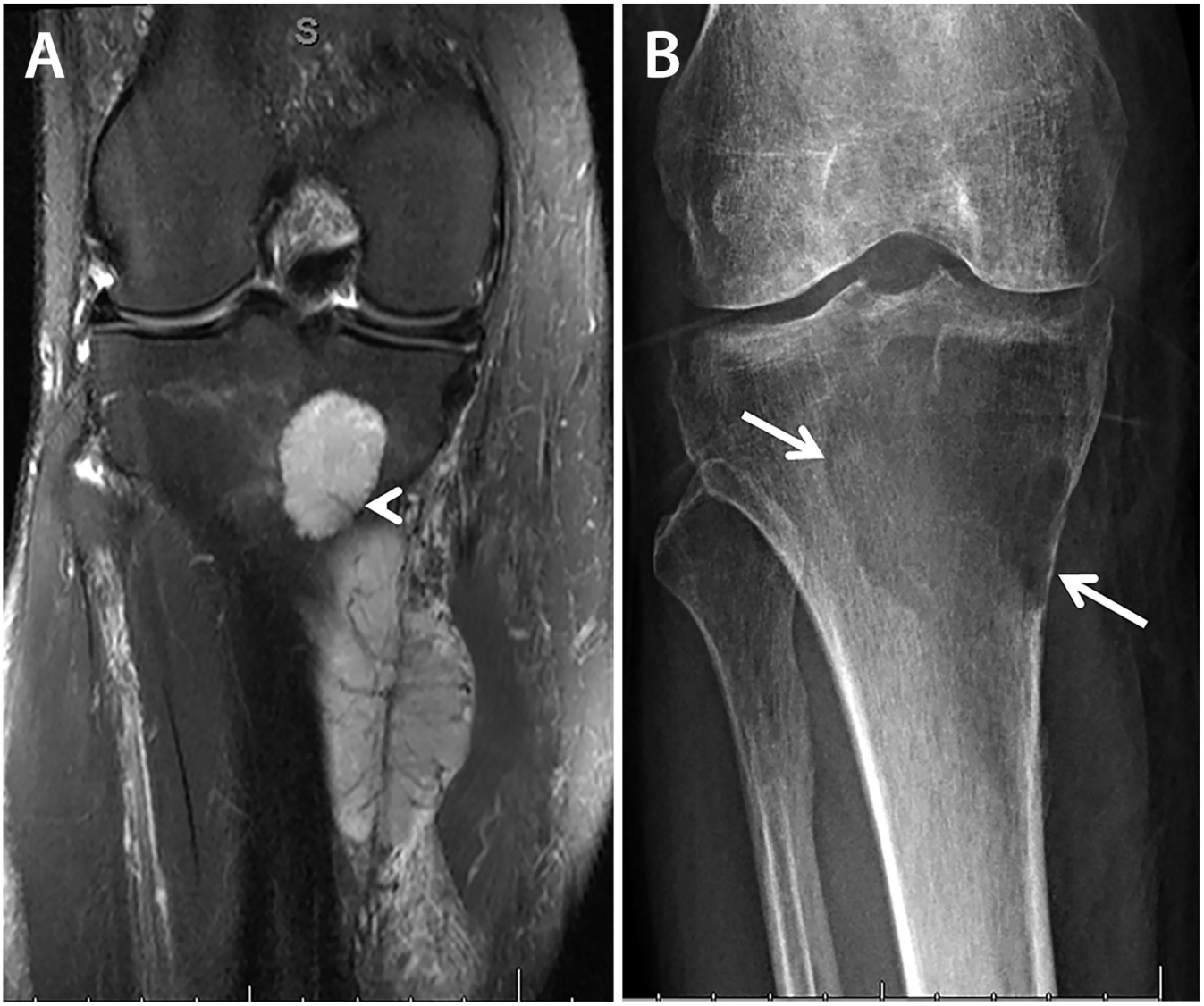

Figure 1.

Case 1, radiologic findings, preoperative and post neoadjuvant therapy. A) Preoperative coronal fat-saturated T2-weighted MRI image demonstrates heterogeneous hyperintensity in both intra- and extra-osseous components with a small perforating vessel at the posterior medial margin of the tibia (arrowhead) that may have allowed spread of the tumor between intraosseous and extraosseous components. The tumor vasculature in the soft tissue component is arborizing and hypointense. B) Radiograph of the tumor after neoadjuvant therapy shows a lytic lesion in the subarticular region of the proximal tibia, with sharp but non-sclerotic margins laterally, and a more poorly defined inferior margin. High-grade endosteal scalloping of the proximal tibia is present medially.

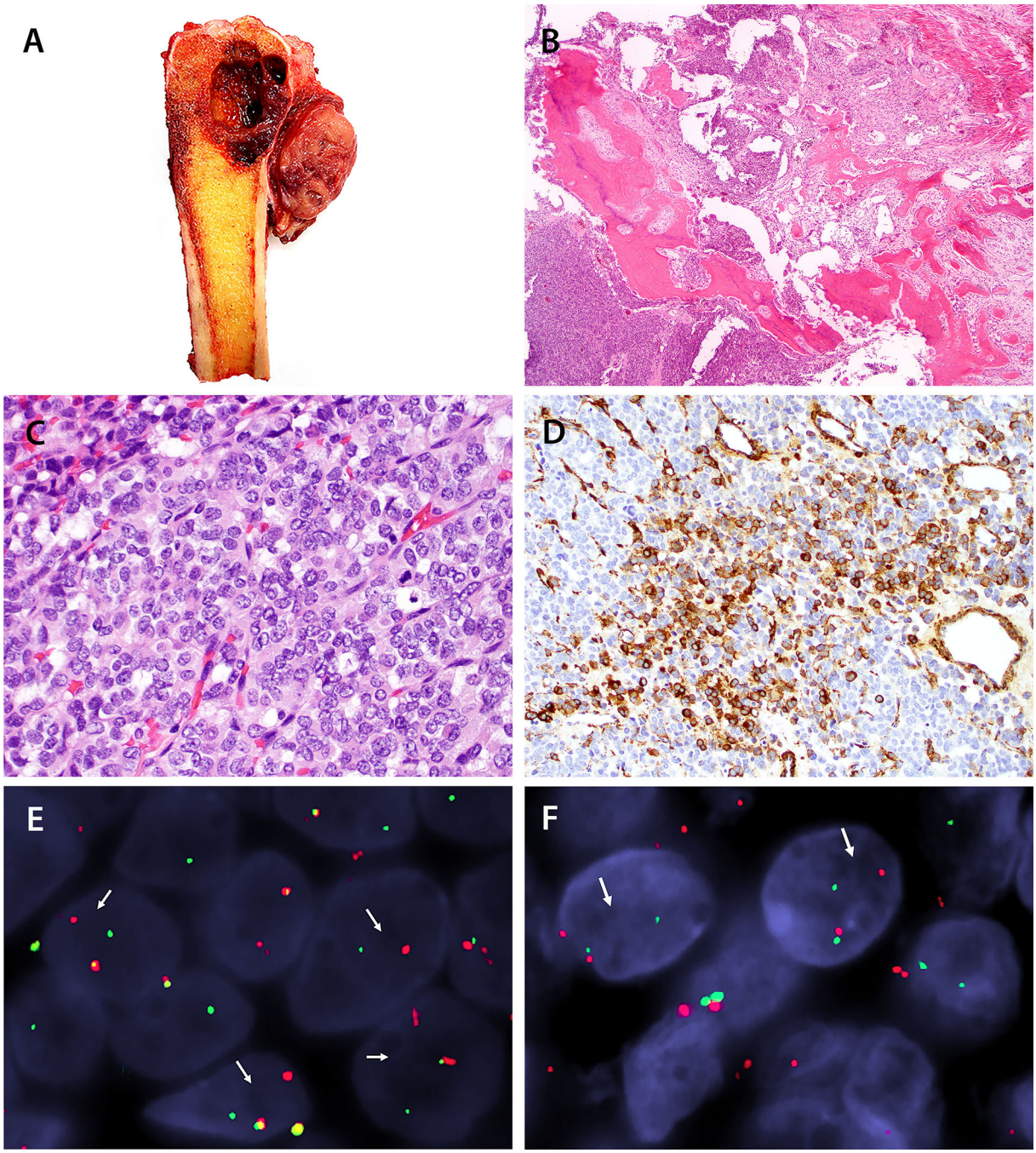

Figure 2.

Case 1, pathologic findings. A) Gross examination of the resected distal tibia shows a red-white, hemorrhagic tumor with a predominant cystic component within the medullary cavity and a pink-tan fleshy component within the adjacent soft tissue. B) A low-power histologic section demonstrates that tumor is present within the medullary cavity as well as infiltrating the cortex, and it extends into adjacent periosteum with prominent associated periosteal woven bone deposition (40x, H&E). C) On high power, the tumor is composed of packets of small blue cells arranged in trabeculae. The neoplastic cells demonstrate ovoid nuclei,

vesicular chromatin, and scant lightly eosinophilic cytoplasm. Mitotic figures are present (400x, H&E). D) A subset of tumor cells is positive for smooth muscle actin (SMA) by immunohistochemistry (200x, immunohistochemical stain). E) Fluorescence in-situ hybridization (FISH) confirms rearrangement of the *ACTB* locus by break-apart probe (red, centromeric; green, telomeric). F) FISH confirms *GLI1* break apart (red, centromeric; green, telomeric).

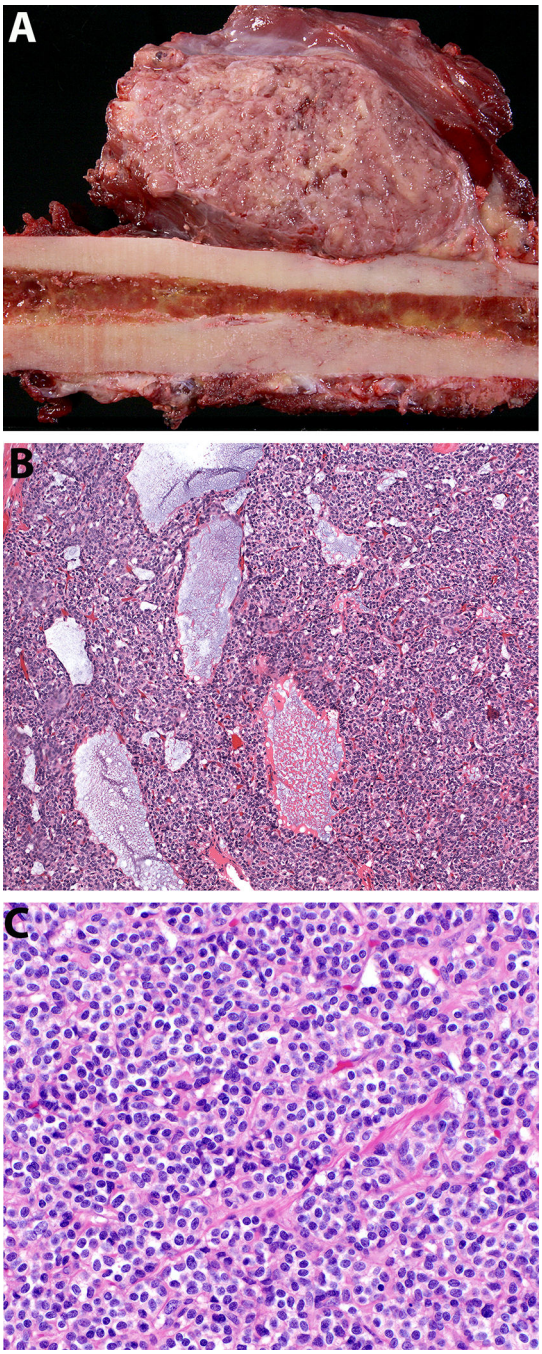

Figure 3.

Case 2, pathologic findings. A) Gross examination of the resected thigh metastasis shows a well-demarcated, soft, red-white ovoid mass within skeletal muscle that focally erodes the adjacent cortex of the femur. B) On low power, the neoplastic cells are arranged in small groups with a delicate background vasculature and foci of myxoid stroma (100x, H&E). A high-power image shows a proliferation of cytologically uniform small cells with round-to-ovoid nuclei, dispersed chromatin, and small nucleoli with variably distinct cell borders (400x, H&E).

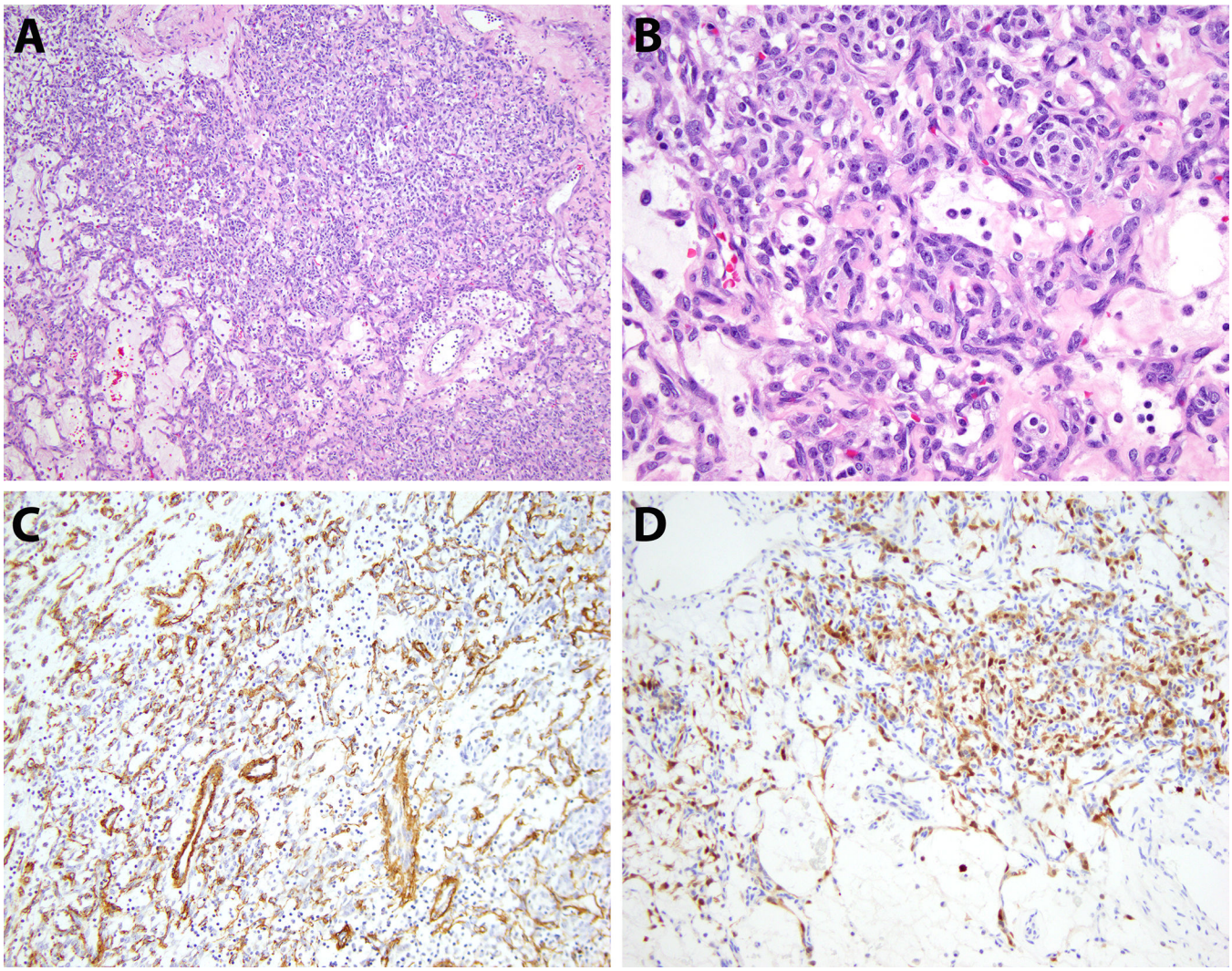

Figure 4.

Case 3, pathologic findings. A) Low-power view of the ovarian tumor shows neoplastic cells arranged predominantly in sheets with areas of alternating cellularity (100x, H&E). B) Cytologic features demonstrate bland-appearing ovoid tumor cells with scant cytoplasm and a vascular-rich stroma (400x, H&E). C,D) The tumor cells express SMA (focal) and S100 protein by immunohistochemistry (200x, immunohistochemical stains).

Table 1:

Patient demographics and tumor pathologic features

	Sex	Age	Tumor site	Tumor size	Mitotic index	Vascular invasion	Necrosis (pretreatment)
# 1	F	57	Right tibia	9.8 cm	5/10 HPF	Y	N
# 2	M	62	Right scapula	7.5 cm	1/50 HPF	Y	N
# 3	F	41	Left ovary	7.0 cm	1/50 HPF	N	Y (focal)

Abbreviations: F: female; Y: yes; N: no; HPF: high power fields.

Table 2:

Imunohistochemical profiles of each tumor

	SMA	MSA	Desmin	S100	EMA	Pan- Keratin	CD99	WT-1	CD10	Ki-67
# 1	+ (f)	+ (r)	−	−	+ (w, f)	−	+ (w, f)	−	−	35%
# 2	+/+ (f)	+ (f)	−	−	−	−	+/−	−	NP	NP
# 3	+ (f)	−	−	+ (f)	+	+	−	−	+	1%

Abbreviations: (f), focal; (r), rare cells; (w), weak; NP: not performed; x/x, different results between initial and subsequent specimens. Refer to the main text for a complete description of all immunohistochemistry performed.

Table 3:

Clinicopathologic features of tumors with *ACTB-GLI1* gene fusions, including previously and currently reported cases

Case # (year)	Author	Sex	Age	Tumor Site	Size (cm)	Clinical Presentation	Histology and Assessment of Biologic Potential	IHC features	Treatment	Follow-up (months)
1–5 (2004)	Dahlen et al[1]	M	61	Calf	2.0	N/A	Spindle-to-ovoid; homogenous, arranged around thin-walled blood vessels; infiltrative/ lobular growth; 3/5 focal myxoid stroma; 2/5 subendothelial protrusion into vascular lumina. Benign.	+SMA, EMA (f) −Desmin, S100, CK	Resection	Died of unrelated causes, NED (60) *
	Dahlen et al[1]	F	27	Tongue	0.8	N/A		+SMA −Desmin, S100, CK, EMA	Neoadjuvant chemo + resection	NED (60)
	Dahlen et al[1]	M	11	Tongue	5.0	N/A		+SMA (f) −Desmin, S100, CK, EMA	Neoadjuvant chemo + resection	NED (22)
	Dahlen et al[1]	F	65	Stomach	5.5	N/A		+SMA (f) −Desmin, S100, CK, EMA	Resection	NED (24)
	Dahlen et al[1] (previously reported)[10]	F	12	Tongue	2.4	Growing tongue mass		+SMA (f) −Desmin, S100, CK	Resection	NED (120)
6 (2012)	Bridge et al[2]	M	67	Bone (talus)	2.7	Pain in right foot and ankle	Spindle-to-ovoid; cellular, prominent lesional vasculature; focal myxoid stroma; invasive growth. Low-grade malignant on biopsy, benign on excision.	+SMA (f), EMA (f) −Desmin, S100, CK	Amputation	NED (204) *
7 (2016)	Castro et al[3]	F	9	Stomach	6.9	Abdominal pain and vomiting	Ovoid-to-spindle; plexiform vasculature, cystic, circumscribed with lymphoid capsule, ischemic necrosis. Biologic potential not specified.	+EMA (f) −Desmsin, SMA, CK, S100	Partial gastrectomy	NED (6)
8–11 (2018)	Antonescu et al[4]	M	20	Thigh	N/A	N/A	Round to epithelioid; arranged in nests, cords, and reticular patterns; mostly solid, occasional myxoid stroma. Biologic potential malignant based on clinical.	+S100 −SMA, CK, EMA	N/A	N/A
	Antonescu et al[4]	F	30	Foot	1.5	N/A		+S100 −SMA, CK, EMA	N/A	AWD, LN met (21)
	Antonescu et al[4]	F	79	Retrope-ritoneum	N/A	N/A		−S100, SMA, CK, EMA	N/A	AWD, LN met (interval N/A)
	Antonescu et al[4]	F	38	Chest wall (muscle)	N/A	N/A		+CK (f)	N/A	N/A

Case # (year)	Author	Sex	Age	Tumor Site	Size (cm)	Clinical Presentation	Histology and Assessment of Biologic Potential	IHC features	Treatment	Follow-up (months)
								−S100, SMA, EMA		
12 (2018)	Koh et al[9]	F	11	Ovary	15.0	Abdominal pain and distension	"Round to spindle;" alternating hypo- and hypercellular, cystic, pushing border; necrosis; "rare" mitoses; +subendothelial tumor proliferation. Biologic potential not specified.	+S100 −Desmin, SMA, CK, EMA	Left salpingooph-orectomy	NED (24) *
13–15	Current cases	F	57	Bone (tibia)	9.8	Painless mass	Round-to-ovoid; richly vascularized stroma; myxoid stroma in 1 case. Low-to-intermediate grade malignant.	+SMA (f), EMA (f) −S100, CK, desmin	Neoadjuvant chemo+ resection	AWD, bone met (27)
		M	62	Bone (scapula)	7.5	Palpable mass		+SMA (+/f) −S100, EMA, CK, desmin	Resection + adjuvant radiotherapy	AWD, lung met (84) and soft tissue/ bone met (180)
		F	41	Ovary	7.0	Incidental ovarian cyst	Ovoid; alternating hypo- and hypercellular, solid/ cystic;necrosis. Biologic potential not clear.	+SMA (f), S100 (f), EMA, CK-Desmin	Total abdominal hysterectomy with bilateral salpingooph-orectomy	NED (14)

Abbreviations: IHC, immunohistochemistry; N/A: not available; S100, S100 protein; chemo, chemotherapy; NED, no evidence of disease; AWD, alive with disease; met, metastasis; LN, lymph node.

* per personal communication with prior author(s).